JACS
JOURNAL OF THE AMERICAN CHEMICAL SOCIETY
Communication
pubs.acs.org/JACS

Constructing Two-Dimensional Nanoparticle Arrays on Layered Materials Inspired by Atomic Epitaxial Growth

Hai-Xin Lin,[†,⊥] Liang Chen,[†,⊥] De-Yu Liu,[†,‡] Zhi-Chao Lei,[†] Yu Wang,[†,§] Xiao-Shan Zheng,[†] Bin Ren,[†,§] Zhao-Xiong Xie,[†,§] Galen D. Stucky,*[,‡,§] and Zhong-Qun Tian*[,†,§]

[†]State Key Laboratory of Physical Chemistry of Solid Surfaces and Department of Chemistry, College of Chemistry and Chemical Engineering, Xiamen University, Xiamen 361005, China

[‡]Department of Chemistry and Biochemistry, University of California, Santa Barbara, California 93106, United States

[§]Collaborative Innovation Center of Chemistry for Energy Materials, Xiamen University, Xiamen 361005, China

Supporting Information

ABSTRACT: Constructing nanoparticles into well-defined structures at mesoscale and larger to create novel functional materials remains a challenge. Inspired by atomic epitaxial growth, we propose an "epitaxial assembly" method to form two-dimensional nanoparticle arrays (2D NAs) directly onto desired materials. As an illustration, we employ a series of surfactant-capped nanoparticles as the "artificial atoms" and layered hybrid perovskite (LHP) materials as the substrates and obtain 2D NAs in a large area with few defects. This method is universal for nanoparticles with different shapes, sizes, and compositions and for LHP substrates with different metallic cores. Raman spectroscopic and X-ray diffraction data support our hypothesis of epitaxial assembly. The novel method offers new insights into the controllable assembly of complex functional materials and may push the development of materials science at the mesoscale.

In the past decade, much attention has been paid to the chemical synthesis of functional nanoparticles (NPs) with different compositions and morphologies.[1−4] However, NPs usually need further self-assembly or co-assembly with other materials to form composite functional materials for advanced uses.[5−9] Moreover, the performance of the composite material is related not only to its own atomic or nanoscale structures but also to the mesoscale structures in which defects, interfaces, and non-equilibrium processes are more important and complex. Constructing composite materials with well-defined structures at the mesoscale provides rich opportunities to obtain novel functional materials by controllable hierarchical assembly.[10−13]

A two-dimensional gold or silver NP array (Au or Ag 2D NA) is one of the most common assembly patterns with a periodic lattice used in plasmonic devices[14,15] and solar energy conversion.[16,17] Techniques for production of large area 2D NAs, such as the Langmuir−Blodgett technique,[18] slow evaporation method,[19,20] template assembly,[21−23] and particle surface modification with linker molecules (e.g., DNA is often used for precise assembly of NPs),[24−26] have therefore been in development. However, the as-prepared 2D NA is difficult to transfer onto the desired substrates, and during the direct co-assembly of gold or silver NPs with other materials, multilayered assembly often occurs, which will compromise the performance of the 2D NA in the functional structure. It is highly desirable to develop new methods to construct 2D NA composites by directly assembling NPs on the functional substrates, which will allow better control of the interface structures and reduction of mesoscale defects.

The concepts of assembling NPs are usually analogous to the crystallization process of molecules where the nanoparticles are considered as artificial atoms.[27,28] From this point of view, assembling NP monolayers onto a specific surface has common ground with the molecular level epitaxial growth process. Beyond the interaction between NPs for assembly, the substrate−building block interactions are more important for the epitaxial process. Given the epitaxial growth model (Frank−van der Merwe model), the interaction energy among atoms in the deposited overlayer should be weaker than that between the overlayer and the substrate. In addition, the lattice mismatch should be within a few percent; otherwise, island growth (Volmer−Weber (V−W) model) or an intermediate type of growth (Stranski−Krastanow model) would occur[29,30] (Figure S1a,b). When the NPs are used as the building blocks, the forces between the NPs mainly depend on the interaction between the surface-modified molecules, and the lattice match mainly depends on whether the molecular assembly layer on nanoparticles matches the lattice of the substrate. For layered materials (substrate), by functionalizing the NPs with one component of those materials while using the other components to tune the interaction between surface molecules on NPs and the substrate, it is possible to achieve NP "epitaxial assembly" as an analogue of the atomic epitaxial growth (Figure 1).

In this research, we use the seed-growth method to synthesize noble metal nanoparticles capped by cetyltrimethylammonium bromide (CTAB), a widely used cationic surfactant. The molecule contains one halogen ion that adsorbs on the metal surface and one quaternary ammonium (CTA^+) that forms double layers by the hydrophobic effect.[31] To achieve assembly similar to an epitaxial growth process, functionalized substrates containing a CTA^+-like structure are highly preferred to reduce the lattice mismatch. Therefore, we selected a class of widely studied materials called layered hybrid perovskites (LHPs),

Received: January 4, 2015
Published: February 11, 2015

DOI: 10.1021/ja5128538
J. Am. Chem. Soc. 2015, 137, 2828−2831

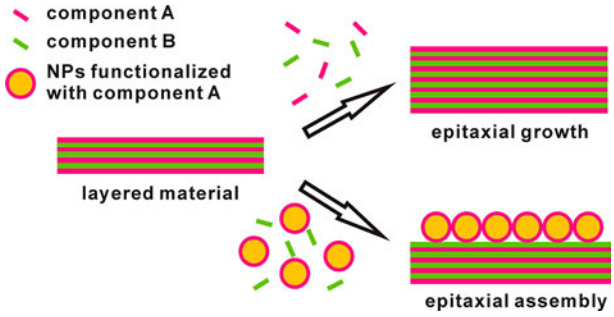

Figure 1. Schematic of the proposed epitaxial assembly strategy compared to epitaxial growth.

which can be synthesized by the direct reaction of the halogen quaternary ammonium salt with a metal halide (MX_2, M = Cd, Pb, Cu, etc., X = Cl, Br, I). Each coordination octahedron of the metal cation contains six halide ions, and they are connected as a planar inorganic backbone layer; the long-chain hydrophobic organic layer interacts with the inorganic layer by the electrostatic interaction.[32] Because of the similarity between LHPs and the CTAB capping layer on Au NPs, Au NPs could assemble onto the LHP material composed by CTAB, expected to take advantage of plasmonic properties from the ordered Au NP array to obtain composite functional materials (Figure S1c,d).

In the synthesis, the $CdCl_2$ aqueous solution was added to the gold colloidal solution containing excess CTAB. A silky luster was observed immediately which is attributed to the light scattering of CTAB–Cd microsheets (CTAB–Cd MS) (Figures 2a and S3). The excess free CTAB in the mixture solution was

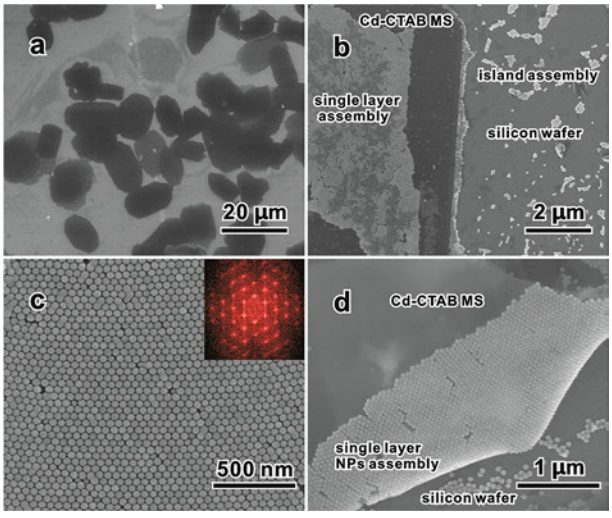

Figure 2. SEM images of (a) CTAB–Cd MS without NPs; (b) spherical Au NPs on a CTAB–Cd MS and on silicon wafer under low magnification; (c) single-layer hexagonal close-packed spherical Au NP array on the CTAB–Cd MS under high magnification; inset is fast Fourier transform; (d) spherical Au NPs assembled on a bent microsheet.

removed by centrifugation. The redispersed suspension was drop-casted onto a hydrophilic silicon chip and then dried under vacuum. Nanopaticles are assembled onto the microsheet during the drying process. The solvent evaporation (entropic force) acts as the driving force of the assembly.[33,34] A schematic of the procedure is shown in Figure S2 (experimental details are given in the Supporting Information).

In sharp contrast with the silicon surface, Au NPs form a large area 2D close-packed array with very few defects on the CTAB–Cd MS (Figure 2c), which is highly ordered with long-range uniform orientation (Figures 2b and S1d). NPs only randomly disperse on the silicon (Figures 2b and S1c), which is consistent with the island growth model (V–W mode). More interestingly, NPs can even be well-assembled onto a bent microsheet (Figure 2d), and this serves as additional proof that the formation of a uniform 2D array of NPs should be attributed to the strong interaction between NP and CTAB–Cd MS.

Furthermore, nonspherical NPs with various shapes (Figure 3) can also form 2D arrays through this method. Au octahedrons,

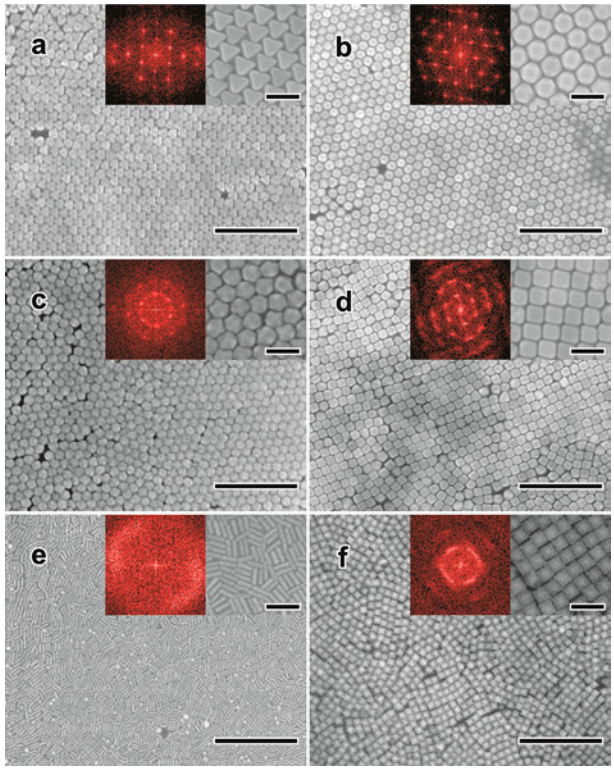

Figure 3. SEM images of two-dimensional nanoparticle arrays with different building blocks on CTAB MS: (a) Au octahedron; (b) Au truncated nanocube; (c) Au trisoctahedron; (d) Au nanocube; (e) Au nanorod; (f) (backscattered electron mode) Au@Pd nanocube assembled on LHP. Insets are fast Fourier transforms and zoomed-in images correspondingly. The scale bars are 500 nm for the main image and 100 nm for the insets.

Au truncated cubes, and Au trisoctahedrons tend to form the hexagonal close-packed arrays (Figure 3a–c). Among them, the octahedron and truncated cube show a long-range translation order, whereas the trisoctahedron has anisotropy larger than that of spherical particles, which is less favorable for hexagonal close packing, which results in more defects and much smaller assembled domains with translation symmetry. Although the Au nanocube and nanorod are not greatly energetically favorable to form a hexagonal close-packed array, they can still form random or glassy close-packed monolayers (Figure 3d,e). For the Au@Pd nanocube, though its composition and electron affinity are different from those of the Au NPs, the single-layer close-packed 2D array can be formed, as well (Figure 3f).

One of the main causes of defects is the existence of nonuniform NPs. The defect-free assembly can be achieved with a high-quality colloid with uniform NPs. With the increase in

DOI: 10.1021/ja5128538
J. Am. Chem. Soc. 2015, 137, 2828–2831

number of the nonuniform NPs, self-similar assembling phenomenon will occur (Figure S4). As both cases in Figure 2 and Figure 3 show, this assembly method is applicable to NPs with different shapes, sizes (Figure S5), and compositions. This suggests that the assembly phenomenon is dominated by the interaction of surfactant molecules on the substrate and NPs' surfaces rather than interactions from the metallic NP surface directly.

To further prove our "epitaxial assembly" hypothesis, IR, Raman spectroscopies, and X-ray diffraction (XRD) were used to determine the layered structure of CTAB−Cd MS. IR and Raman spectra of CTAB and CTAB−Cd MS (Figure S6) indicate that CTAB is one of the main components of the CTAB−Cd MS. For the Raman spectrum of the microsheet, an intense peak at 161 cm^{-1} was observed in the low wavenumber region, but the counterpart of this peak was not observed for CTAB crystals (Figure 4a). This peak belongs to the Cd−Br bond, which indicates that Cd ions are incorporated in the CTAB−Cd MS by the formation of Cd−Br bonds.[35] Further structure analysis of the CTAB and the microsheet through XRD patterns shows that they both have uniformly spaced diffraction peaks, demonstrating the layer structure (Figure 4b). On the diffraction pattern of the CTAB−Cd MS sample, some minor peaks corresponding to excess CTAB as a separated phase (blue dashed lines) were also found. It may be the reason why fully covered assembly cannot be achieved on the CTAB−Cd MS (Figure S8). The distance between layers was calculated from the XRD patterns by Bragg's equation. For CTAB, the distance is 2.60 nm, which is close to the thickness of the CTAB double layer.[36] For CTAB−Cd MS, the distance is 3.04 nm, larger than that of CTAB. This shows that the Cd^{2+} ions are intercalated between CTAB layers.

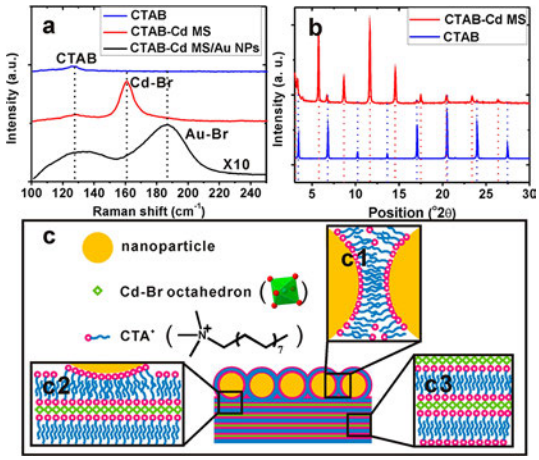

Figure 4. (a) Raman spectra of CTAB and CTAB−Cd MS with and without assembled Au NPs. (b) XRD patterns of CTAB and CTAB−Cd MS. (c) Presumed structure of a 2D NP array on the CTAB−Cd MS. The enlarged detail view (c1) between NPs; (c2) between NP and CTAB−Cd MS; (c3) inside CTAB−Cd MS. The freestanding Br^- ions and the Br^- ions adsorbed on the NPs, which keep the assembly electroneutral, are not shown.

Raman spectra in the low wavenumber region further reveal more interactions at the molecule level. The Raman spectrum of the CTAB−Cd MS with Au NPs assembled differs from that of bare CTAB−Cd MS in the low wavenumber region (Figure 4a). For the CTAB−Cd MS with Au NPs, a new peak at 188 cm^{-1}, which belongs to Au−Br bonds, emerges due to the specific adsorption of the bromine ions onto the Au NPs.[37] In addition, the peak at 161 cm^{-1} disappears, which belongs to the Cd−Br bond. This can be explained by the very strong surface-enhanced Raman scattering on Au NPs (especially in hot spots due to the plasmonic coupling) that suppressed the signal from CTAB−Cd MS. Thus, the signal mainly comes from the Au−Br bonds in the hot spots.[38] Besides that, the Au NP layer will diminish the signal, so the Cd−Br band can be even more invisible. This result also suggests that there are no Cd ions between Au NPs (Figure 4c1). The presumed structure of the CTAB−Cd MS is shown in Figure 4c3, which is similar to other LHP structures.[39] According to all characterization data, the overall structure of the assembly with NPs on the CTAB−Cd MS is illustrated as Figure 4c2. This model states a hybrid structure between the molecule and NPs, with the CTAB molecule as the bridge between them.

This model of a 2D NA on the LHP is very similar to the typical epitaxial growth of crystals in two key respects. First, CTAB molecules attached to the Au NPs become the external part of the LHP with excellent structural affinity. Second, metal ions are only intercalated between the CTA^+ layers of LHP, which increases the electrostatic interactions inside the LHP as well as between NPs and LHP, whereas the adsorption structure between the Au NPs remains a hydrophobic interaction (Figure S7). When the interaction energy between the NPs is weaker than that between the NPs and the LHP substrate, a similar assembly process for epitaxial growth occurs, which we call an "epitaxial assembly". After NPs form a single layer, excess NPs possibly further assemble on the first-layer nanoparticle array, while on the silicon wafer, they tend to aggregate in smaller regions, similar to an island growth mode (Figure S8). In control experiments without metal ions, NPs cannot assemble on the CTAB crystal and tend to mix with it (Figure S9). Besides, LHP can be dissolved in a large quantity of water and is at precipitation−dissolution equilibrium in our system. Therefore, although the interaction between NPs and substrate is strong, it may still provide a reversible dynamic assembly process, which is advantageous to minimize the energy requirement of guiding building blocks and form a uniform close-packed structure during this process. These may be the reasons why nanoparticles favor forming the ordered two-dimensional assembly on this LHP.

This epitaxial assembly method has several advantages for constructing complex functional materials. First, it has good universality: on one hand, our method should be applicable for most monodispersed CTAB-capped NPs; on the other hand, our procedure is also universal for LHP materials with different metal cations. For example, the Cu ion can be used to replace the toxic Cd ion, and a similar 2D NA is also obtained on CTAB−Cu LHP materials (Figure S10). Second, through the direct assembly of a 2D NA with desired functional substrates, it does not need a time-consuming transfer step, which may damage the 2D NA and cause defects. Third, according to our experimental results, the 2D NA is chemically bound to LHP substrates, which makes it a perfect mesoscale interface and further reduces defects.

In conclusion, inspired by conventional crystalline epitaxial growth, we have developed a novel method to obtain two-dimensional NP arrays of large area with few defects directly on the LHP microsheets. The method is time-saving and universal. These composites are expected to combine both the properties of nanoparticles and LHP materials and provide application potential in light-emitting diodes[40] and solar cells.[41−43] This epitaxial assembly strategy will provide new ideas to control the self-assembly of NPs and co-assembly with other layered

DOI: 10.1021/ja5128538
J. Am. Chem. Soc. 2015, 137, 2828−2831

functional materials in the creation of more complex, multifunctional composite materials at the mesoscale.

■ ASSOCIATED CONTENT

Supporting Information

Experimental details and additional data. This material is available free of charge via the Internet at http://pubs.acs.org.

■ AUTHOR INFORMATION

Corresponding Authors

stucky@chem.ucsb.edu
zqtian@xmu.edu.cn

Author Contributions

⊥These authors contributed equally.

Notes

The authors declare no competing financial interest.

■ ACKNOWLEDGMENTS

Financial support from the National Science Foundation of China (Grant Nos. 21321062, 21033007, 91427304), Ministry of Science and Technology Foundation of China (Grant No. 2015CB932300), and the U.S. National Science Foundation (Grant No. DMR-0805148) is gratefully acknowledged. We thank Prof. Nan-Feng Zheng for helpful discussions. D.-Y.L. is especially grateful for the use of MRL facilities. The MRL Shared Experimental Facilities are supported by the MRSEC Program of the NSF under Award No. DMR 1121053, a member of the NSF-funded Materials Research Facilities Network (www.mrfn.org).

■ REFERENCES

(1) El-Sayed, M. A. *Acc. Chem. Res.* **2004**, *37*, 326.
(2) Tao, A. R.; Habas, S.; Yang, P. D. *Small* **2008**, *4*, 310.
(3) Xia, Y. N.; Xiong, Y. J.; Lim, B.; Skrabalak, S. E. *Angew. Chem., Int. Ed.* **2009**, *48*, 60.
(4) Zhang, L.; Niu, W. X.; Xu, G. B. *Nano Today* **2012**, *7*, 586.
(5) Balazs, A. C.; Emrick, T.; Russell, T. P. *Science* **2006**, *314*, 1107.
(6) Zhang, H.; Liu, Y.; Yao, D.; Yang, B. *Chem. Soc. Rev.* **2012**, *41*, 6066.
(7) Li, Z. T.; Zhu, Z. N.; Liu, W. J.; Zhou, Y. L.; Han, B.; Gao, Y.; Tang, Z. Y. *J. Am. Chem. Soc.* **2012**, *134*, 3322.
(8) Shevchenko, E. V.; Talapin, D. V.; Murray, C. B.; O'Brien, S. *J. Am. Chem. Soc.* **2006**, *128*, 3620.
(9) Tang, Z.; Wang, Y.; Podsiadlo, P.; Kotov, N. A. *Adv. Mater.* **2006**, *18*, 3203.
(10) Whitesides, G. M.; Boncheva, M. *Proc. Natl. Acad. Sci. U.S.A.* **2002**, *99*, 4769.
(11) Velev, O. D.; Gupta, S. *Adv. Mater.* **2009**, *21*, 1897.
(12) Wang, T.; Zhuang, J. Q.; Lynch, J.; Chen, O.; Wang, Z. L.; Wang, X. R.; LaMontagne, D.; Wu, H. M.; Wang, Z. W.; Cao, Y. C. *Science* **2012**, *338*, 358.
(13) Whitesides, G. M.; Grzybowski, B. *Science* **2002**, *295*, 2418.
(14) Nie, Z. H.; Petukhova, A.; Kumacheva, E. *Nat. Nanotechnol.* **2010**, *5*, 15.
(15) Tao, A.; Sinsermsuksakul, P.; Yang, P. D. *Nat. Nanotechnol.* **2007**, *2*, 435.
(16) Mubeen, S.; Lee, J.; Lee, W. R.; Singh, N.; Stucky, G. D.; Moskovits, M. *ACS Nano* **2014**, *8*, 6066.
(17) Atwater, H. A.; Polman, A. *Nat. Mater.* **2010**, *9*, 205.
(18) Tao, A. R.; Huang, J. X.; Yang, P. D. *Acc. Chem. Res.* **2008**, *41*, 1662.
(19) Bigioni, T. P.; Lin, X. M.; Nguyen, T. T.; Corwin, E. I.; Witten, T. A.; Jaeger, H. M. *Nat. Mater.* **2006**, *5*, 265.
(20) Wen, T. L.; Majetich, S. A. *ACS Nano* **2011**, *5*, 8868.
(21) Zhou, Y.; Zhou, X. Z.; Park, D. J.; Torabi, K.; Brown, K. A.; Jones, M. R.; Zhang, C.; Schatz, G. C.; Mirkin, C. A. *Nano Lett.* **2014**, *14*, 2157.
(22) Pavan, M. J.; Shenhar, R. *J. Mater. Chem.* **2011**, *21*, 2028.
(23) Hellstrom, S. L.; Kim, Y.; Fakonas, J. S.; Senesi, A. J.; Macfarlane, R. J.; Mirkin, C. A.; Atwater, H. A. *Nano Lett.* **2013**, *13*, 6084.
(24) Shen, Z. R.; Yamada, M.; Miyake, M. *J. Am. Chem. Soc.* **2007**, *129*, 14271.
(25) Ofir, Y.; Samanta, B.; Rotello, V. M. *Chem. Soc. Rev.* **2008**, *37*, 1814.
(26) Senesi, A. J.; Eichelsdoerfer, D. J.; Macfarlane, R. J.; Jones, M. R.; Auyeung, E.; Lee, B.; Mirkin, C. A. *Angew. Chem., Int. Ed.* **2013**, *52*, 6624.
(27) Lu, Z. D.; Yin, Y. D. *Chem. Soc. Rev.* **2012**, *41*, 6874.
(28) Zhuang, J. Q.; Wu, H. M.; Yang, Y. G.; Cao, Y. C. *J. Am. Chem. Soc.* **2007**, *129*, 14166.
(29) Fan, F. R.; Liu, D. Y.; Wu, Y. F.; Duan, S.; Xie, Z. X.; Jiang, Z. Y.; Tian, Z. Q. *J. Am. Chem. Soc.* **2008**, *130*, 6949.
(30) Bauer, E.; van der Merwe, J. H. *Phys. Rev. B* **1986**, *33*, 3657.
(31) Nikoobakht, B.; El-Sayed, M. A. *Langmuir* **2001**, *17*, 6368.
(32) Mitzi, D. B. *J. Chem. Soc., Dalton Trans.* **2001**, *1*, 1.
(33) Ming, T.; Kou, X. S.; Chen, H. J.; Wang, T.; Tam, H. L.; Cheah, K. W.; Chen, J. Y.; Wang, J. F. *Angew. Chem., Int. Ed.* **2008**, *47*, 9685.
(34) Young, K. L.; Personick, M. L.; Engel, M.; Damasceno, P. F.; Barnaby, S. N.; Bleher, R.; Li, T.; Glotzer, S. C.; Lee, B.; Mirkin, C. A. *Angew. Chem., Int. Ed.* **2013**, *52*, 13980.
(35) Macklin, J. W.; Plane, R. A. *Inorg. Chem.* **1970**, *9*, 821.
(36) Paradies, H. H.; Clancy, S. F. *Rigaku J.* **2000**, *17*, 20.
(37) Wang, H.; Levin, C. S.; Halas, N. J. *J. Am. Chem. Soc.* **2005**, *127*, 14992.
(38) Camden, J. P.; Dieringer, J. A.; Wang, Y. M.; Masiello, D. J.; Marks, L. D.; Schatz, G. C.; Van Duyne, R. P. *J. Am. Chem. Soc.* **2008**, *130*, 12616.
(39) Ricard, L.; Cavagnat, R.; Rey-Lafon, M. *J. Phys. Chem.* **1985**, *89*, 4887.
(40) Dohner, E. R.; Hoke, E. T.; Karunadasa, H. I. *J. Am. Chem. Soc.* **2014**, *136*, 1718.
(41) Zhang, W.; Saliba, M.; Stranks, S. D.; Sun, Y.; Shi, X.; Wiesner, U.; Snaith, H. J. *Nano Lett.* **2013**, *13*, 4505.
(42) Park, N.-G. *J. Phys. Chem. Lett.* **2013**, *4*, 2423.
(43) Smith, I. C.; Hoke, E. T.; Solis-Ibarra, D.; McGehee, M. D.; Karunadasa, H. I. *Angew. Chem., Int. Ed.* **2014**, *126*, 11414.

DOI: 10.1021/ja5128538
J. Am. Chem. Soc. 2015, 137, 2828−2831